

N96-18719

NDB

52-92

60382

P. 10

NEW INSIGHT IN THE SOLAR T_{MIN} REGION FROM THE CO LINES AT 4.67 MICRON

HAN UITENBROEK and ROBERT W. NOYES

*Harvard-Smithsonian Center for Astrophysics,
60 Garden Street, Cambridge MA 02138, USA*

Abstract. We discuss recent observations of the fundamental vibration-rotation transitions of carbon monoxide (CO) in the solar infrared spectrum. Employing a new array detector at the McMath-Pierce facility on Kitt Peak we find that the CO lines sketch a rich picture of the dynamics of the solar temperature minimum region, the lower boundary of the chromosphere. In a spectra-spectroheliogram and a time-sequence of slit-spectra obtained during exceptional seeing conditions we observe small-scale bright, ring shaped, blueshifted features. We speculate that they are the signature of granular overshoot into the convectively stable temperature minimum. The centers of the rings are among the coolest elements seen in strong CO-line heliograms on the disk, and may be instrumental to the low temperatures observed in CO close to the solar limb.

Key words: CO molecule, temperature minimum, infrared, granulation

1. Introduction

Not many spectral diagnostics are available to study the structure and dynamics of the solar chromosphere. While our knowledge primarily stems from a few strong lines like the hydrogen $H\alpha$ and Ca II H&K lines, most other lines have chromospheric contributions only close to the limb where accurate observations are difficult. Due to this lack of reliable observations we are currently not yet able to tell what the exact nature of the chromosphere is and what causes its temperature to rise from photospheric to (eventually) coronal values. Recent simulations by Carlsson and Stein (these proceedings) for instance suggest that the chromo "sphere" need not exist over the whole surface but rather represents moderately hot material that is locally and intermittently heated by outwardly propagating shock waves. With this in mind it is evident that we need to look for new observations that could confirm or discount the widely different models. It may seem unlikely that observations of molecular carbon monoxide (CO) lines provide us with such an opportunity, since all molecules dissociate at temperatures characteristic for the chromosphere. However, modeling any layer in the atmosphere requires a proper understanding of its boundary conditions. In the case of the solar chromosphere we are particularly interested in the amount of mechanical energy coming from the lower boundary, *i.e.*, the temperature minimum region, and lines of CO may play an important role precisely in diagnosing this energy flux and the form in which it is presented to the chromosphere.

In a static plane-parallel solar model both the balance of CO association and dissociation and the excitation-de-excitation equilibrium of the vibration-rotation transitions are dominated by collisions (Ayres and Wiedemann, 1989). Consequently, all relevant population are in thermodynamic equilibrium with local conditions (LTE),

and intensities map directly into temperatures. Surprisingly enough, CO observations close to the limb require temperatures as low as 3700–3800 K (Noyes and Hall, 1972a; Ayres and Testerman, 1981), values which are much lower than those predicted by models based on almost any other spectral diagnostic. A recently constructed model by Avrett (private communication) illustrates the discrepancy in thermal diagnostics clearly. The model fits disk-center intensities of several hundred CO lines in the ATMOS infrared atlas (Farmer and Norton, 1989), but predicts intensities that are far too low in such prominent spectral features as the Ca II H&K lines and the 150 nm and 100 μm continua which both originate from the same region. This failure of standard one-dimensional models to accommodate CO observations with other spectral diagnostics clearly calls for more intricate models of the solar atmosphere that include spatial inhomogeneities and/or time-dependent behavior. For this we need detailed observations that show when and where in the atmosphere the lowest CO temperatures occur. In Sect. 3 we discuss our continuing effort to do such observations with the McMath-Pierce solar telescope at Kitt Peak. First we briefly discuss the instrumental setup in Sect. 2, while we present our conclusion in Sect. 4.

2. Observational parameters

Infrared CO spectra at 4.67 μm have been available with good spectral resolution for more than twenty years (Noyes and Hall, 1972a; 1972b). Until recently, however, the lack of array detectors has severely limited the spatial resolution that could be achieved at such long wavelengths. This changed with the advent of a new infrared array detector at the NSO McMath-Pierce facility on Kitt Peak. A comprehensive description of the instrument and observational parameters for our first set of observations with the infrared array in October 1993 can be found in Uitenbroek *et al.* (1994). The first results of this run show the CO lines to be very exciting lines rich in information. In this section we briefly mention improvements in the instrumental setup for a second observation run in May 1994. New results are discussed in the next section.

The diffraction limited resolution of the 1.5 m McMath-Pierce main telescope is $0''.77$ at 4.6 μm . The vertical spectrograph with infrared grating and 220 μm wide slit achieves a resolution of $\Delta\lambda/\lambda = 90\,000$. The detector is a 256×256 InSb array with an adjustable readout rate which was usually set to 7 Hz. In our second observing run (May 1994) we used minifying optics to compress the image in the spatial direction and expand the field of view by a factor of two to approximately $100''$ with a $0''.38$ /per pixel resolution. Addition of an optical disk allowed us to increase the data throughput of the system and achieve a cadence of 2 seconds per frame, an improvement of more than a factor of 2 over the first observations in October 1993.

In Fig. 1 we display a sample spectrum of a quiet-Sun region on the disk (cosine of the viewing angle $\mu = 0.5$). This spectral region represents one of the few infrared windows through the earth atmosphere with little contamination of terrestrial lines. It contains several strong and weak (*i.e.* low and high excitation) lines. We will use the 3-2 R14 in this window as representative for stronger CO lines, and the 7-6 R68

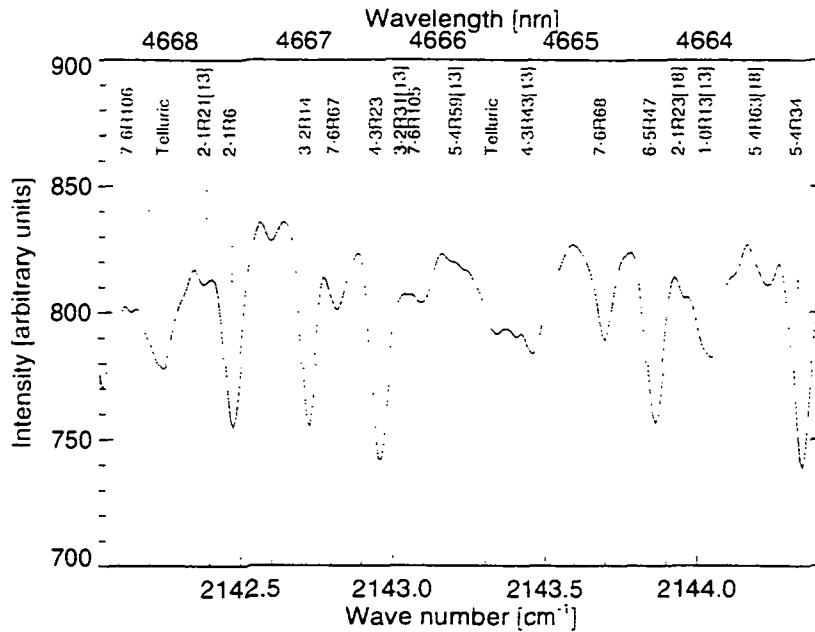


Fig. 1. A sample solar CO spectrum from a quiet area at $\mu = 0.5$. Lines marked with [13] refer to lines from the $^{13}\text{C}^{18}\text{O}$ isotope; those marked with [18] to lines that arise from $^{12}\text{C}^{18}\text{O}$.

line as representative for weaker lines because they are relatively less blended with other lines.

We used the instrument in two different modes of observation: one stresses resolution in space, the other resolution in time. In the first mode we scanned the solar surface with the slit to build spectra-spectroheliograms, data cubes that allow us to make two-dimensional spatial maps of any function of wavelength such as the intensity in a stretch of continuum, the core of a certain line, or a line's Doppler shift. In the second mode we took time-sequences of spectra at a fixed position on the surface and recorded temporal variations of spectral quantities along the slit. To construct line-intensity maps and Doppler maps we made parabolic fits to the lowest three points of the line profile at each position of a space-space or space-time scan, and determined the value at and the position of the minimum of the fitted profile. Doppler shifts in the displays of Figs. 2—4 are specified with respect to the average position of the line, with blue shift (corresponding to upward mass motion) coded light and redshift coded dark.

3. Results

The picture of the temperature minimum region that emerges from time and space resolved spectroscopy of the infrared CO lines is a very dynamical one. Our first observations with the infrared array (Uitenbroek *et al.*, 1994) showed that, at disk center, line shifts variations have a dominant period of 5 minutes, spatial scales of 10–20'', and typical RMS amplitudes of 0.3–0.4 km/s. Line-core intensities of the stronger lines exhibit more the character of the chromospheric 3-minute oscillations with a smaller spatial scale of 3–5'', and RMS variations that correspond to 90 K

temperature fluctuations. Higher up in the temperature minimum region the spatial distribution of temperatures appears asymmetric with an extended tail towards small-scale cold elements. The magnetic network could be tentatively identified (as bright elements) in the intensity maps, but this could not be substantiated since we did not have co-spatial Ca II K line images during the October 1993 run. The network did not seem to have a clear signature in maps of line shift.

We now turn to a discussion of two sets of observations that were obtained on May 6, 1994 under very favorable seeing conditions. Judging from the smallest scale elements in our data the atmospheric seeing must have been at the diffraction limit of the telescope at $4.67 \mu\text{m}$ or better. The telescope was positioned on a quiet area at heliographic position 12N, 62E (corresponding to a viewing angle of 60 degrees, or $\mu = 0.5$) with an East-West oriented slit. We first obtained a time-sequence of 1200 spectra at 2.2 second intervals and then obtained a $100'' \times 100''$ spatial scan (200 spectra at $0''.5$ spacing) centered on the surface position of the preceding time-sequence. Between the time-sequence and the spectra-spectroheliogram we obtained a co-spatial Ca II K-line filtergram with a wide bandpass centered on the core of the line. This allows us now to unambiguously identify network elements.

Figure 2 shows three space-time maps extracted from the time-sequence of spectra. It contains two maps of temperature fluctuations as derived from continuum intensity variations (left panel) and variations in 3-2 R14 line-core intensity (middle panel) respectively, and a space-time map of 3-2 R14 line-core shift (right panel). In order to do justice to the high spatial and temporal resolution of the present data we display only the first half of the sequence. At around 6 and 22 minutes after the start of the sequence clouds passed over giving rise to the dark bands which are especially visible in the low contrast continuum map (left panel, Fig. 2). In the line-shift map the passing clouds cause a temporary loss of resolution. Because the left side of the slit was oriented towards the (East) limb the continuum map shows the effect of limb darkening towards that end, while the difference in projection of solar rotation velocity in the line of sight between both sides of the slit ($\approx 0.2 \text{ km/s}$) gives rise to a Doppler map that is, on average, slightly darker (*i.e.* more red shifted) on the left (limb-ward) side.

The bright vertical lines at horizontal positions $33''$ and $64''$ in the continuum and line intensity maps of Fig. 2 are network elements. They are easy to identify in the K-line filtergram (upper left panel Fig. 4). The location of the network is not readily identified in the Doppler map. Compared to our previous observations (Uitenbroek *et al.*, 1994, Fig. 3 therein) we note several important differences. The favorable seeing conditions allow us to see a fine-scale pattern with structures as small as $1''$, that reminds us of the photospheric granulation: bright streaks that last for several minutes and that sometimes diverge, sometimes converge. The streaks, which often appear in pairs correspond to blueshifted material in the Doppler map, where they sometimes seem to merge into more fuzzy blobs of blue-shifted (coded bright here) material. Since the spectrograph slit renders a one-dimensional cross-section of the solar surface, the streaks most likely represent ring shaped (although not necessarily circular) structures. The typical separation of $3\text{-}5''$ of the bright streaks is slightly larger than the cell size of photospheric granulation, but corresponds perhaps to the strongest granules overshooting in the stable temperature minimum

region. These appear as "exploding" granules in photospheric granulation movies (Title *et al.*, 1989). In between the bright streaks there are sometimes dark single streaks that last for about 2 minutes. These intermediate dark narrow elements are among the darkest elements in the time-sequence, reminiscent of the centers of large granules that cool strongly due to the adiabatic expansion of upflowing material in the exponentially stratified atmosphere in theoretical granulation simulations (*e.g.* Stein and Nordlund, 1989). It is likely that a similar picture as seen in CO line intensity is observed in the spectra of the Ca II K-line wings that originate from the same altitude. We are reminded of the effect, first observed by Evans and Catalano (1972), in which granulation contrast inverts between K-line wing intensities and continuum intensity where granular centers are bright.

We remark that the peak-to-peak temperature variations of approximately 400 K seem to differ little between observations with very different seeing conditions (*cf.* the lower left panel in Fig. 3 of Uitenbroek *et al.*, 1994, and the middle panel of Fig. 2). Thus, we do not expect real fluctuations to be much larger. By contrast, the peak-to-peak velocity variations at the viewing angle of $\mu = 0.5$ of the present data are a factor of 2 higher than those observed at disk center under less favorable seeing conditions. This indicates that either small-scale velocity variations partially cancel out when the image is blurred, or that the velocity distribution is strongly dependent on viewing angle. The latter would mean that horizontal velocities would be larger than vertical. Although this does not conform with measured microturbulence (which is a proxy for the average small-scale velocity fields) derived from photospheric lines which shows exactly the opposite behavior (*cf.*, Rutten and Milkey, 1979), it agrees with simulations of solar granulation which show strong expansion flows in horizontal directions (Steffen and Muchmore, 1988; Stein and Nordlund, 1989). (Further observations, of course, will resolve this issue.)

The time slices in Fig. 2 display a lot of detail that make them difficult to analyze. They represent a superposition of at least two modulating phenomena: the granulation with small spatial scales and time-scales of up to 10 minutes, and the response of the temperature minimum region to the global 5-minute P-mode oscillations. We attempted to separate these effects by filtering the time-slices in space and time. The result is displayed in Fig. 3 where the bottom two panels show the time-slices of temperature variation (left panel) and line shift (right panel) of the 3-2 R14 line filtered with a temporal passband of 3-5 minutes and spatial low-pass filter with a cutoff at $10''$. The top two panels were constructed by removing the bottom two slices λ from the total signal as displayed in the middle and right panels of Fig. 2.

Correlating the two 3-5 minute band slices we find that redshift leads maximum temperature by 50 seconds (*i.e.*, approximately 90 degrees in phase, as expected for an adiabatic standing wave). Note that the distribution of line shifts in the lower right image is symmetric around zero, while that of the upper right slice is skewed to larger positive values (blue shift). These have a relatively small filling factor since the zero level is defined as the average velocity over the whole slice. The topology of the "granulation" slice, therefore, has small areas with relatively strong blue shift embedded in larger areas of relatively mild redshift. Most sharply defined blueshifted areas correlate with bright areas in the 3-2 R14 temperature map, although there

is not a well-defined one-to-one correspondence. This may be due to the relatively large viewing angle of 60 degrees which causes considerable projection effects.

After the time-sequence displayed in Fig.2 we obtained a K-line filtergram and CO spectra-spectroheliogram of the same area. Figure 4 shows three spatial maps extracted from the heliogram, which was centered on the slit position of the time-sequence. The corresponding subarea of the K filtergram is shown in the lower right panel with the slit position of the preceding time-sequence overplotted. The other three panels of Fig. 4 display the 3-2 R14 temperature map (upper left panel), continuum temperature map (upper right), and the 3-2 R14 Doppler shift map (lower left). The continuum and 3-2 R14 maps are all co-spatial and simultaneous on a horizontal line-by-line basis; it takes 440 seconds to build up the whole heliogram scanning the slit over the surface. The K-line filtergram appears to be considerably more blurred than the CO heliograms, probably due to the worse seeing at the shorter wavelength of the K line.

Some bright patches of network appear in the temperature heliograms. Their position is easily confirmed from the K-line filtergram. The brightest two in the middle of the images correspond to the bright vertical stripes in the temperature maps of Fig.2. Confirming our earlier remark, the network is not recognized in the 3-2 R14 Doppler map (lower left panel). The Doppler map is characterized by small scale bright (blue-shifted) patches of 2-3'' size, and a larger scale checker-board pattern of 15-20''. The latter is characteristic of the 5-minute oscillation.

It is difficult to recognize the ring-shaped patterns suggested by the space-time maps in the heliograms. This may be due to a fragmentation of overshooting granules that is also visible as a break-up of exploding granules in photospheric movies (Title *et al.*, 1989). Ideally we would like to be able to obtain series of heliograms at small enough time intervals to confirm our impressions. Unfortunately, the current setup does not allow the required high data rate.

4. Conclusion

We were fortunate to encounter very favorable seeing conditions during part of our May 1994 observation run. The obtained CO data reveal an even more intricate picture of the temperature minimum region than we suspected from our previous infrared array observations. A time-sequence that we obtained shows bright streaks associated with blue-shifted material. We tentatively identify the ring-like structures that the streaks imply with the signature of granular flow. We would like to remark that the picture we sketch is not in conflict with the topology of granular flow as sketched by Stein and Nordlund (1989) who describe the top layer of the granulation flow as having broad, slow, up-flow regions and confined fast down flows. The latter picture refers to the situation beneath the photosphere, invisible to us at any wavelength. Rather, we speculate that in CO we observe occasionally strong granules that overshoot into the stable temperature minimum region and give rise to localized up-flow regions, which appear sometimes as ring-shaped temperature enhancements, sometimes as bright blobs in the temperature maps, embedded in a more uniform medium that is dominated by the 3-5 minute oscillations. In this picture the rapidly expanding granule interiors give rise to small scale cold areas

that appear as dark streaks lasting for 1-2 minutes in CO time slices. These cold areas could play an important role in the low CO temperatures that are observed at the solar limb by creating a shadowing effect in which they obscure hotter material in the line of sight due to their larger CO abundance.

Acknowledgements. We would like to thank Doug Rabin and Dave Jaksha for help with the observations, and Gene Avrett for fruitful discussions. This work was supported in part through NASA grant NAGW-2545. H.U. thanks the University of Oslo for making it possible to attend the workshop in Oslo.

References

- Ayres, T. R. and Testerman, L.: 1981, *Astrophys. J.* **245**, 1124
Ayres, T. R. and Wiedemann, G. R.: 1989, *Astrophys. J.* **338**, 1033
Evans, J. W. and Catalano, C. P.: 1972, *Sol. Phys.* **27**, 299
Farmer, C. B. and Norton, R. H.: 1989, *A High-Resolution Atlas of the Infrared Spectrum of the Sun and the Earth Atmosphere from Space*, NASA Ref. Pub. 1224, Vol 1
Noyes, R. W. and Hall, D. N. B.: 1972a, *Bull. Am. Astron. Soc.* **4**, 389
Noyes, R. W. and Hall, D. N. B.: 1972b, *Astrophys. J. Lett.* **176**, L89
Rutten, R. J. and Milkey, R. W.: 1979, *Astrophys. J.* **231**, 277
Steffen, M. and Muchmore, D.: 1988, *Astron. Astrophys.* **193**, 281
Stein, R. F. and Nordlund, Å.: 1989, *Astrophys. J. Lett.* **342**, L95
Title, A. M., Tarbell, T. D., Topka, K. P., Ferguson, S. H., Shine, R. A., and the SOUP Team: 1989, in R. J. Rutten and G. Severino (Eds.), *Solar and Stellar Granulation*, NATO ASI Series C-263, Kluwer, Dordrecht, p. 225
Uitenbroek, H., Noyes, R. W., and Rabin, D. M.: 1994, *Astrophys. J. Lett.* in press

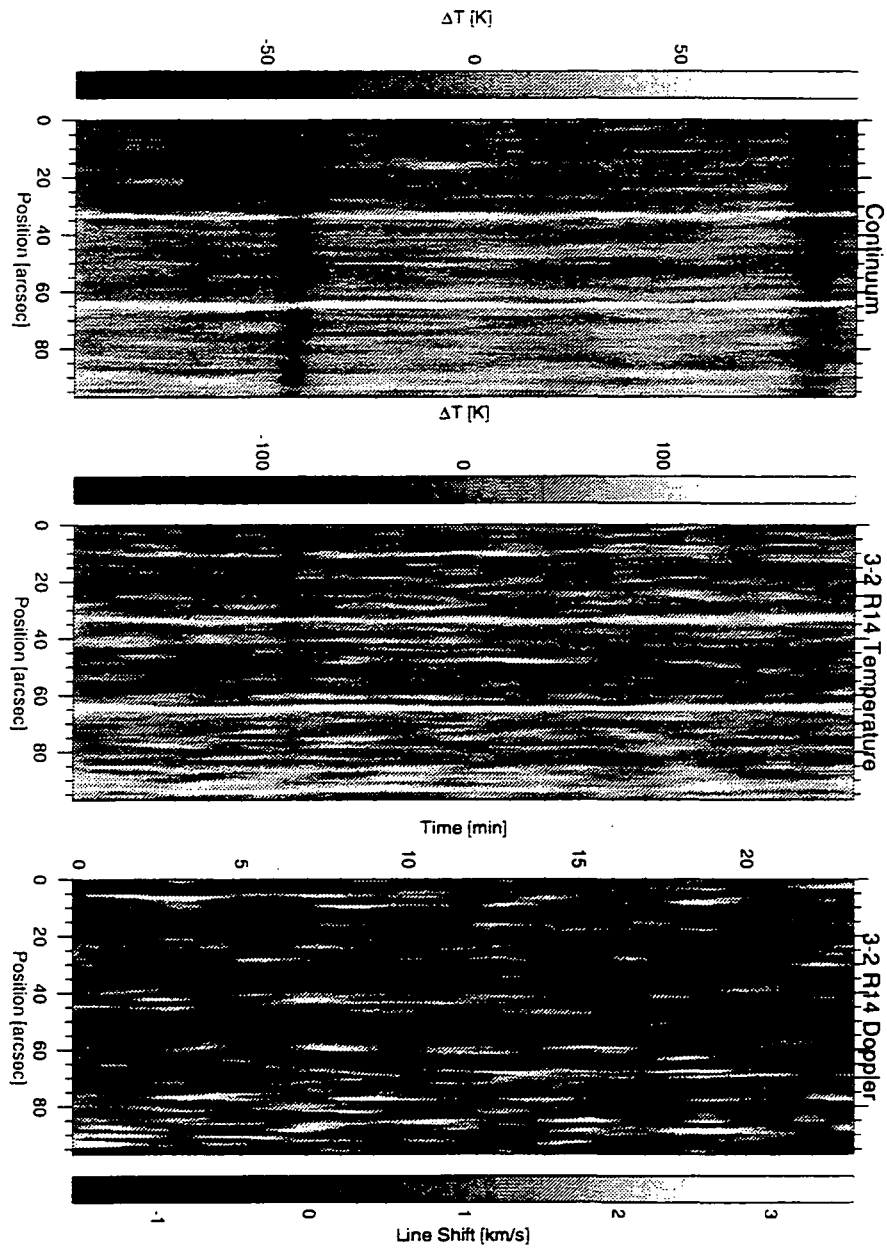


Fig. 2. Space-time maps of infrared continuum variations (left panel), and 3-2 R14 line-core temperature and line-shift variations (middle and right panels respectively).

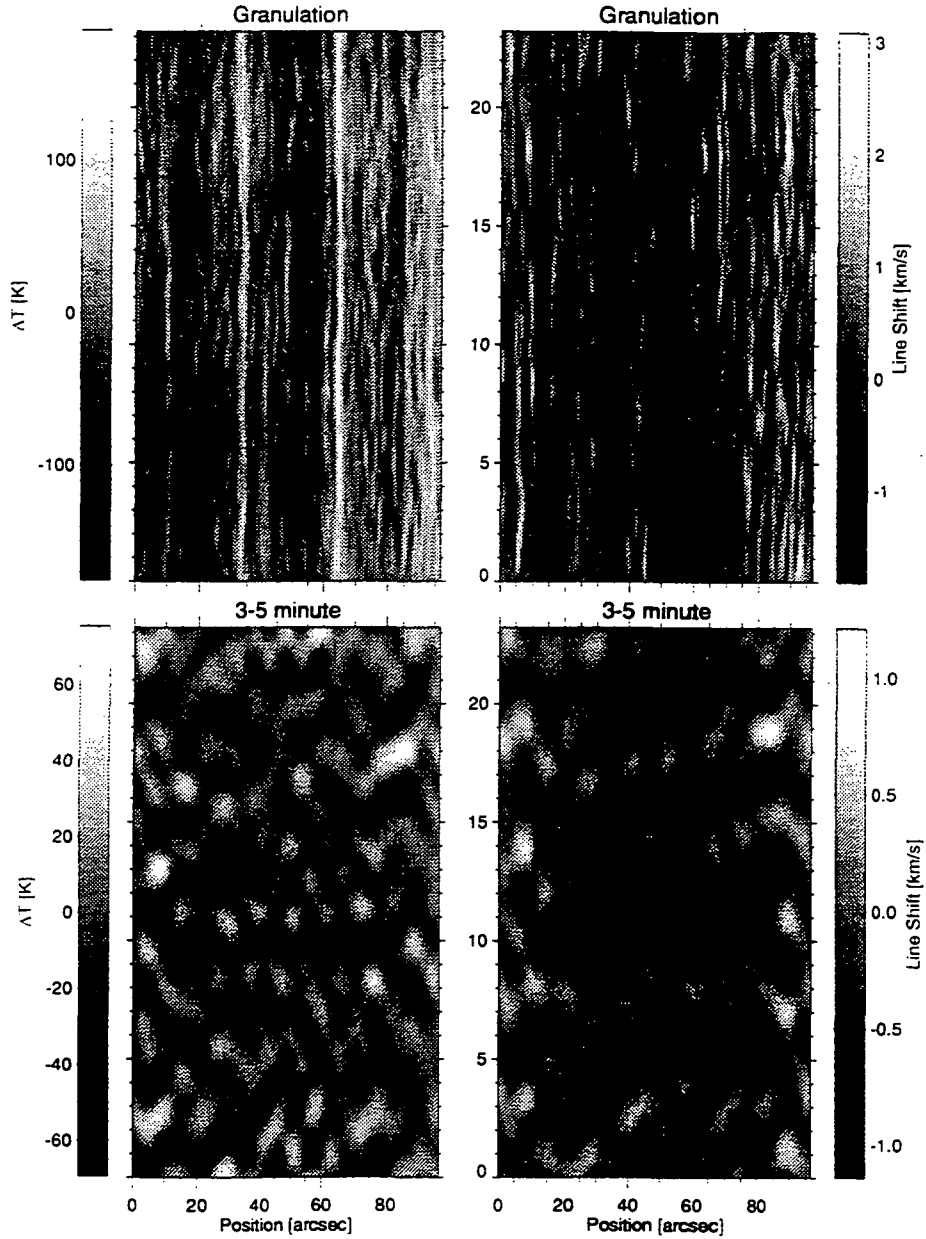


Fig. 3. Filtered time-slices of the 3-2 R14 temperature (left panels) and line shift (right panels) variations. Lower panels are filtered with a 3-5 minute temporal bandpass and a spatial lowpass filter with $10''$ cutoff. Upper panels show slices more characteristic for the spatial and temporal behaviour of granulation with 3-5 minute band removed.

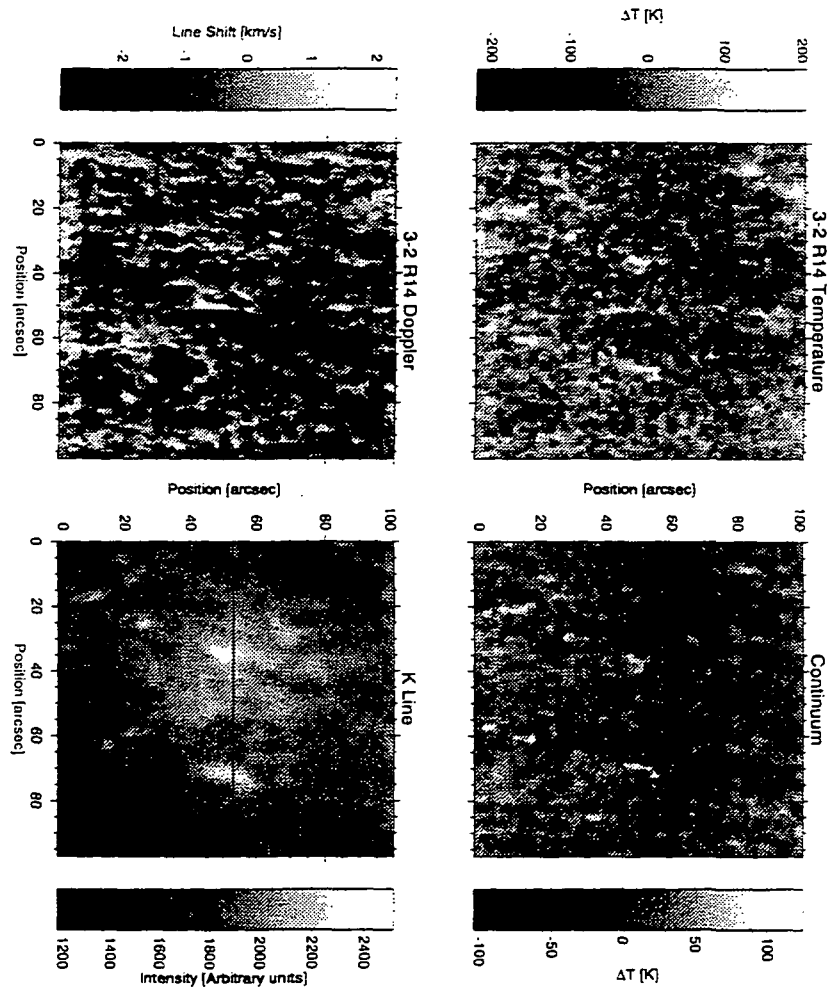


Fig. 4. Heliograms of Ca II K-line core intensity (lower right panel), infrared continuum temperature variations (upper right), 3-2 R14 line shift (lower left), and 3-2 R14 line-center temperature variations (upper left panel). Horizontal line in the K-line filtergram indicates the position of the slit for the preceding time-sequence (see Fig. 2).